Temperature Variation over East Asia during the Lifecycle of Weak Stratospheric Polar Vortex

SUNG-HO WOO

School of Environmental Science and Engineering, Pohang University of Science and Technology, Pohang, South Korea

BAEK-MIN KIM

Division of Climate Change, Korea Polar Research Institute, Incheon, South Korea

JONG-SEONG KUG

School of Environmental Science and Engineering, Pohang University of Science and Technology, Pohang, South Korea

(Manuscript received 19 November 2014, in final form 18 March 2015)

ABSTRACT

The authors investigate the circulation change during the life cycle of a weak stratospheric polar vortex (WSV) event and its impact on temperature variation over East Asia. The lower-tropospheric temperature over East Asia strongly fluctuates despite the slow decay of stratospheric circulation and the continuously negative Arctic Oscillation (AO) pattern during the WSV event. The temperature fluctuation is critically influenced by the variation of the East Asian upper-level coastal trough (EAT), which may be coupled to the stratospheric circulation during the WSV events. The EAT is deepened anomalously during the Peak phase (from lag −5 to lag 5 day) of the WSV, and East Asian temperature is lowest during this phase. During the next period (Decay-1 phase: from lag 6 to lag 16 day), in spite of the slowly decaying WSV condition, the cold temperature anomaly over East Asia is suddenly weakened; this change is caused by a westward-propagating signal of an anticyclonic anomaly from the North Pacific to East Asia. After about two weeks (Decay-2 phase: from lag 17 to lag 27 day), the cold conditions over East Asia are restrengthened by an intensification of EAT, which is related to the eastward propagation of a large-scale wave packet originating from a negative North Atlantic Oscillation (NAO)-type structure in the Decay-1 phase and its delayed influence on the East Asia region.

1. Introduction

The stratospheric polar vortex, which is a climatological westerly over the polar cap region, experiences large variability during the boreal winter. The breakdown or abrupt weakening of the polar vortex, especially, which is often called a stratospheric sudden warming (SSW; Matsuno 1971) or weak stratospheric polar vortex (WSV; Baldwin and Dunkerton 2001) event, accompanies the rise of stratospheric temperature and geopotential height (Z) over the polar cap region. Its impact is not just confined within the stratosphere but extends downward to the surface on a time scale of a few weeks (Hartley et al. 1998; Baldwin and Dunkerton 1999, 2001; Hartmann et al. 2000; Thompson et al. 2002; Limpasuvan et al. 2004; Perlwitz and Harnik 2003; Black 2002; Black and McDaniel 2004; Charlton and Polvani 2007; Mitchell et al. 2013). These tropospheric signatures of the downward-propagating anomalies strongly resemble the features of the Northern Hemisphere annular mode (NAM) or the Arctic Oscillation (AO), which are large-scale patterns with out-of-phase fluctuations between polar and midlatitude regions (Thompson and Wallace 1998, 2000; Ambaum and Hoskins 2002; Wang and Chen 2010). Moreover, the AO generally shows a barotropic and zonally symmetric structure from the stratosphere to the lower troposphere (Hartley et al. 1998; Baldwin and Dunkerton 2001;

Corresponding author address: Prof. Jong-Seong Kug, Pohang University of Science and Technology, 77 Cheonggam-ro, Nam-gu, Pohang 790-784, South Korea.
E-mail: jskug1@gmail.com

Thompson et al. 2002; Polvani and Waugh 2004; McDaniel and Black 2005). Therefore, previous studies have mainly focused on the zonally symmetric circulation or hemispheric-scale tropospheric pattern that is dynamically related to the WSV.

Although the hemispheric-scale pattern associated with the WSV is well projected onto the negative AO, the tropospheric adjustment related to the WSV could differ regionally. For instance, synoptic eddies may contribute to the strengthening of tropospheric circulation related to the stratospheric circulation (Taguchi 2003; Domeisen et al. 2013). This relationship implies that spatial variation of synoptic eddy activity may influence regionally different tropospheric coupling with the WSV. Recently, some studies reported the impact of stratospheric circulation on tropospheric blocking (Colucci 2010; Kodera et al. 2013). These studies noted the possibility of regional disparity in the tropospheric adjustment associated with the WSV. However, the regional impacts of the WSV have not been studied extensively, despite its potential importance. Only a few studies have examined the regional impact of the WSV. For example, Kolstad et al. (2010) suggested that the development of lower-tropospheric cold temperatures over Eurasia could be related to the WSV. Tomassini et al. (2012) noted that the blocking signature over the polar area, related to the deceleration of the stratospheric polar vortex, leads to extreme cold spells over northern Europe. Although these studies suggested the dynamical and statistical relations between WSV and regional climate, the impact of large WSV events on the tropospheric circulation over East Asia remains unclear.

Nevertheless, East Asian climate is likely to be largely related to the onset and evolution of WSV events. The East Asian coastal trough (EAT) is a representative climatological feature over East Asia during the boreal winter season. The large-scale sinking motion near the rear of the EAT partly contributes to development of the Siberian high (Ding and Krishnamurti 1987; Zhang et al. 1997; Takaya and Nakamura 2005; Gong and Ho 2002). Cold air over Siberia could be advected southeastward along the lower-level anomalous circulation associated with the deepening of EAT into East Asia (Qiu and Wang 1984; Boyle and Chen 1987; Wang et al. 2009); therefore, the deepening of the EAT is a favorable condition for cold anomalies over East Asia (Jeong and Ho 2005; Woo et al. 2012). The development of the Siberian high and East Asian cold condition related to the deepening of EAT is a well-known precursor of WSV events (Kolstad and Charlton-Perez 2011; Cohen and Jones 2011).

The East Asian climate is also remotely modulated by large-scale variability, such as the AO (Thompson and Wallace 1998; Rigor et al. 2000; Son et al. 2012). The negative phase of the AO is strongly related to the strengthening of the Siberian high and EAT, resulting in anomalous cold weather over Eurasia (Thompson and Wallace 1998, 2000; Ambaum and Hoskins 2002; Gong and Ho 2002; Jeong and Ho 2005; Son et al. 2012). This relationship between AO and East Asian climate may imply that the negative AO-like type response to WSV events in the lower troposphere may modulate the East Asian temperature and circulation. Moreover, recent studies reported on the impact of stratospheric disturbance on the East Asian winter climate. Jeong et al. (2006) and Kim et al. (2009) noted the existence of a precursory signal (negative potential vorticity) in the stratosphere before the occurrence of strong East Asian cold surges. Butler et al. (2014) noted that ENSO impacts over Eurasia, including East Asia, are greatly affected by stratospheric pathways.

Although these studies showed that the climatological features over East Asia can be modulated by changes in stratospheric circulation, it is unclear how regional circulation and temperature over East Asia evolve during the life cycle of the WSV events. The present study examines the temporal evolutions of hemispheric and regional circulations associated with the WSV and their effect on the evolution of regional lower-tropospheric temperature over East Asia.

2. Data and methods

a. Data

One of our aims is to examine the circulation and temperature variations related to the WSV on a subseasonal time scale. However, WSV events in the Northern Hemisphere do not frequently occur (Kolstad et al. 2010; Baldwin and Dunkerton 2001). Therefore, to procure as many WSV events as possible, a long-term dataset that has daily data must be used. The National Centers for Environmental Prediction–National Center for Atmospheric Research (NCEP–NCAR) reanalysis dataset is available for the period from 1948 to the present (Kalnay et al. 1996). Daily mean fields of Z, temperature, and zonal wind are used to analyze circulation change and temperature variation associated with the WSV. The dataset has a horizontal resolution of $2.5° \times 2.5°$ and 17 pressure levels from 1000 to 10 hPa. We analyzed 63 winters (December–March) from 1948/49 to 2010/11. The daily anomaly was obtained by the deviation from smoothed (removing 21-day running mean) daily climatology for the total analysis period.

A daily AO index is used to examine the AO evolution during the WSV event. The index is calculated by

projecting the daily mean 1000-hPa Z anomalies onto the AO loading, which is defined by the leading empirical orthogonal function (EOF) pattern for monthly mean 1000-hPa Z anomalies poleward of 20°N in the Northern Hemisphere. Statistical significance was computed using a two-tailed Student's t test.

b. Detection method of stratospheric weak vortex event

The variability of the stratospheric polar vortex has often been evaluated using the NAM index (e.g., Baldwin and Dunkerton 2001) or polar cap Z anomaly integrated over 65°–90°N (e.g., Cohen et al. 2002). The latter is essentially the same as the canonical NAM index with a significant negative correlation (e.g., Baldwin and Thompson 2009). Following Kolstad et al. (2010), the latter measure, the area-weighted polar cap Z (Z_p) anomaly, is used to detect WSV events. Because the stratospheric Z_p anomaly is negatively correlated to a polar vortex, we use $-Z_p$ anomaly. The time series of $-Z_p$ anomalies at 50 hPa (Fig. 1a) shows large short-term variability (intraseasonal-to-interannual time scale) but no apparent long-term trend. The onset of the WSV event is defined as the first day on which the $-Z_p$ anomaly at 50 hPa is lower than its 10th percentile (-292.4 m), and the ending day is defined as the last day of a continuous period during which the $-Z_p$ anomaly at 100 hPa is lower than its -0.5 standard deviation during the winter. If a new day when the $-Z_p$ anomaly at 50-hPa is lower than its 10th percentile occurs during the life cycle of individual WSV events, then we would regard the two events as a single WSV event. Based on this approach, 48 WSV events were identified (Fig. 1); that is, about 0.76 events per winter, which is slightly higher than the frequency of major SSW events, which is about 0.50 events per winter based on the WMO definition. More than 70% of WSV events were classified as major SSW events (Butler et al. 2014). The lower frequency of WSV events in the 1990s compared to other decades is also well detected, in the definition of this study, as SSW events detected in previous studies (Charlton and Polvani 2007; Reichler et al. 2012; Mitchell et al. 2013).

3. Results

To validate the detection of WSV events, we first investigate the temporal evolution of circulation over the polar cap region (north of 65°N) during WSV events (Fig. 1b). The positive Z_p anomalies are prominent in the stratosphere for more than a month. They start to develop at lag -10 day and reach the maximum value at lag 3 day. After the peak, the positive anomalies slowly decay over time. Most of these anomalies were
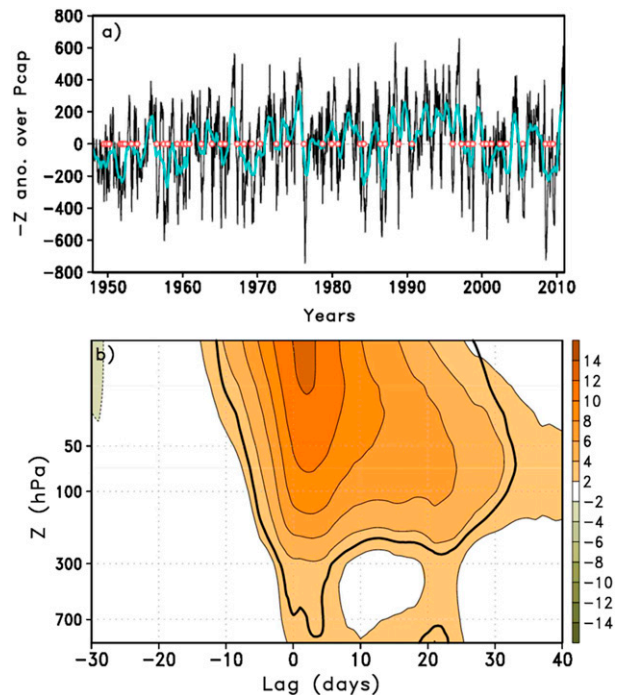

FIG. 1. (a) The Z anomalies (m) averaged northward of 65°N at 50 hPa and their 121-day moving average (blue line). Red circles are WSV events detected in this study. (b) A lead–lag composite of Z anomalies averaged northward of 65°N before and after the starting date of a WSV event (lag 0 day). The Z anomaly in each vertical level is normalized by its standard deviation. The thick black contour is the 95% confidence level.

statistically significant at the 95% confidence level. Significant anomalies are also observed near the surface around lag 0 and 20 days (Fig. 1b); this implies that the tropospheric anomalies are coupled with the stratospheric anomalies. This persistence of stratospheric anomalies and downward coupling to the troposphere correspond to results documented in previous studies (e.g., Baldwin and Dunkerton 2001; Limpasuvan et al. 2004; Charlton and Polvani 2007).

Moreover, during the life cycle of a WSV event (from lag -5 to lag 30 day), the stratospheric spatial pattern shows a zonally symmetric positive Z anomaly over the polar cap and a negative Z anomaly over midlatitudes (Fig. 2), which are well-known features (Limpasuvan et al. 2004; Kolstad and Charlton-Perez 2011). The composite pattern shows the barotropic feature between the lower stratosphere (50 hPa) (Fig. 2a) and upper troposphere (300 hPa) (Fig. 2b). This barotropic feature implies that the stratospheric circulation during WSV events is coupled with the tropospheric circulation. The barotropic structure was particularly strongest in the Arctic, North Pacific, and North Atlantic basins. In addition, negative Z anomalies over East Asia exhibit
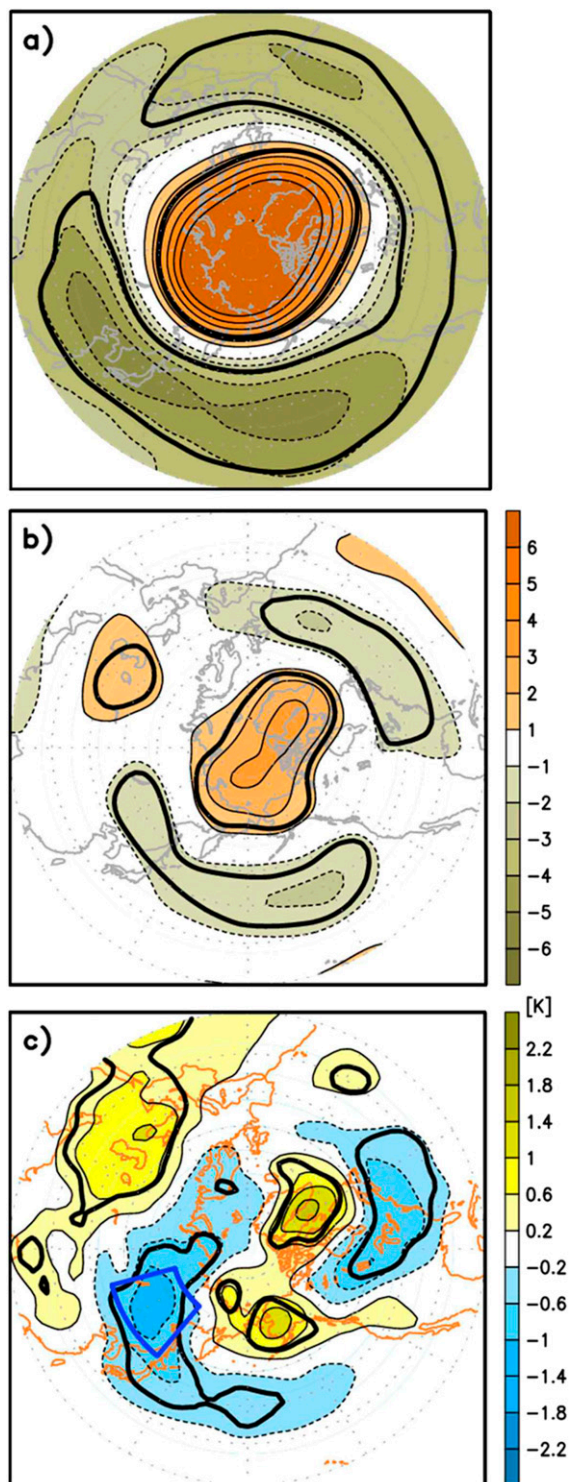
FIG. 2. Composite maps of normalized Z anomalies at (a) 50 and (b) 300 hPa, and (c) the temperature anomaly at 850 hPa during the life cycle of a WSV event (from lag −5 to lag 30 day). The thick black line is the 95% confidence level.

a distinctive barotropic structure. These features make us suggest that tropospheric circulation during a WSV event affects regions differently. In this study, we will focus on the regional tropospheric circulation change and temperature variation related to the WSV, especially over East Asia.

a. East Asian cold condition during WSV events

To examine the effects of WSV events on the lower-tropospheric temperature, composites of temperature at 850 hPa (Fig. 2c) were obtained during the WSV period (from lag −5 to lag 30 day). In spite of the zonally symmetric pattern of stratospheric circulation changes associated with the WSV event, the tropospheric temperature responses are quite zonally asymmetric. The warm anomalies appear over the Arctic area, including Greenland and the Bering Sea, whereas the cold anomalies appear over northern Eurasia and the eastern United States. In particular, the cold anomaly over East Asia was strongest in the Northern Hemisphere. This feature may imply East Asia is one of the regions that is strongly affected by stratospheric circulation changes (Baldwin and Dunkerton 2001; Kolstad et al. 2010).

To examine a relationship between the temporal evolution of the WSV and the East Asian temperature during the life cycle of a WSV event, we carried out the lead–lag composites of the lower-stratospheric Z anomalies (Fig. 3a) and the lower-tropospheric temperature averaged over the polar cap region and East Asia (45°–65°N, 105°–140°E) (Fig. 3b), respectively. It is interesting that the temperature anomaly fluctuates distinctively within the WSV period (Fig. 3b) despite the monotonic variation of the stratospheric signal with just one peak (Fig. 3a). Specifically, the cold anomaly is stronger between lag −10 and lag 5 day, and is weakened rapidly afterward. However, the cold signal is re-strengthened near lag 20 day, and is weakened slowly thereafter. Note that this temperature fluctuation has a longer time scale than that of synoptic eddies. This temperature fluctuation is also unlikely to be a result of chance because 48 WSV events were used to obtain the composite.

To explain this temperature fluctuation during the life cycle of the WSV event, we first investigated the relation to the AO, which manifests its negative phase in the troposphere during the WSV event by the downward signal from the stratosphere. Figure 3c shows the composite of the daily AO index during the life cycle of the WSV events. We found that the temperature fluctuation is not fully explained by the AO (Fig. 3c). The AO index decreases abruptly at about lag −10 day; it generally retains the negative phase without large fluctuation during the WSV event. Moreover, its peak appears after
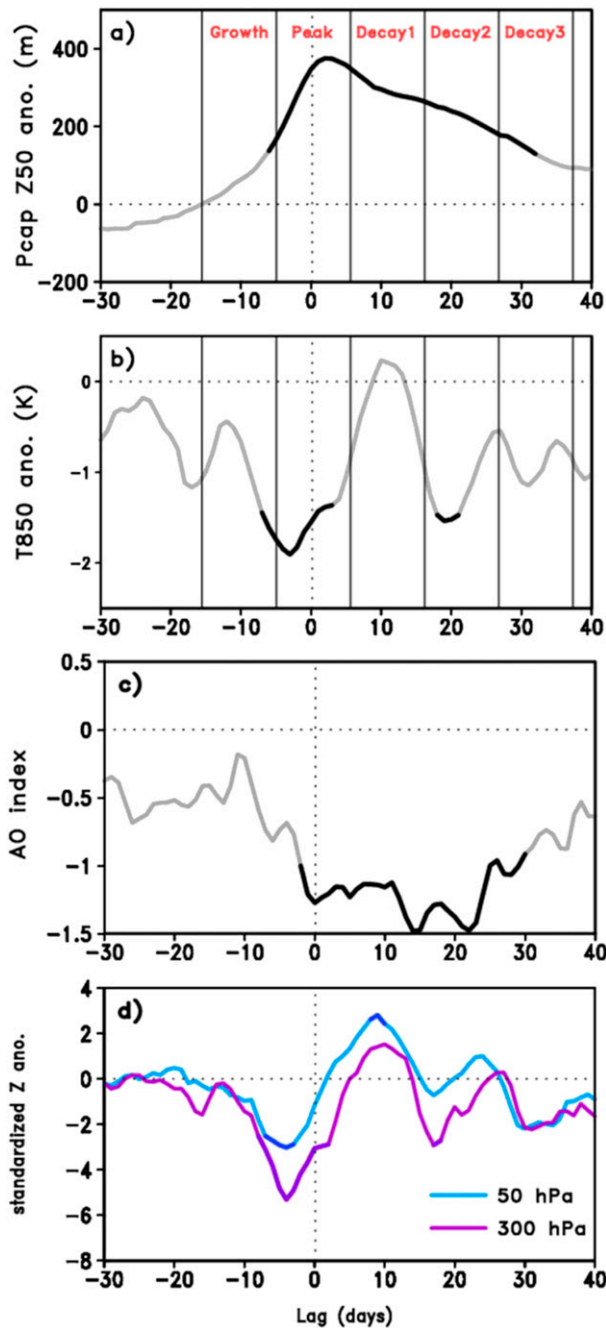
FIG. 3. (a) A lead–lag composite of the Z anomaly averaged northward of 65°N at 50 hPa. (b) A lead–lag composite of temperature (K) at 850 hPa averaged over East Asia (blue box in Fig. 2c) before and after the onset of a WSV event (lag 0 day). (c) A lead–lag composite of the AO index. Thick black lines in (a)–(c) are the 95% confidence levels. (d) A lead–lag composite of the Z anomaly at 50 (light blue) and 300 hPa (light violet) averaged over East Asia. Thick dark blue and thick dark violet lines in (d) are the 95% confidence levels at 50 and 300 hPa, respectively.

lag 10 day. This pattern indicates that the AO is not the main cause of temperature fluctuation over East Asia during the WSV event.

This temperature fluctuation is strongly related to the variation of the upper-tropospheric Z anomaly over East Asia, which roughly measures the strength of the EAT. The variation of EAT is strongly related to the East Asian winter monsoon (EAWM) dominating the temperature variation over East Asia in the winter season (Qiu and Wang 1984; Boyle and Chen 1987; Jeong et al. 2005; Takaya and Nakamura 2005; Wang et al. 2009). Actually, the lag composite of the upper-tropospheric Z anomaly over East Asia (Fig. 3d) shows a similar fluctuation pattern to the temperature anomaly. These features imply that regional tropospheric circulation may contribute to this temperature evolution, rather than zonally symmetric circulation, such as a negative AO pattern. It is interesting that this variation of upper-tropospheric circulation is likely to be regionally related with the stratospheric circulation over East Asia. The evolution of stratospheric circulation averaged over East Asia shows qualitatively similar fluctuation with the upper-tropospheric circulation (Fig. 3d), in contrast with the monotonic variation of the zonal mean stratospheric circulation (Fig. 3a). Although the regional covariation between the stratospheric and tropospheric circulation does not indicate that the stratospheric circulation over East Asia regionally causes the variation of the tropospheric circulation, it can suggest a possibility that the stratospheric variation is regionally connected to the upper-tropospheric circulation over East Asia, which results in the fluctuation of East Asian temperature during the life cycle of the WSV event.

Therefore, to identify dynamic processes associated with the temporal evolution of temperature and circulation over East Asia during the life cycle of the WSV event, we defined five 11-day subperiods (or phases): Growth (from lag −16 to lag −6 day), Peak (from lag −5 to lag 5 day), Decay-1 (from lag 6 to lag 16 day), Decay-2 (from lag 17 to lag 27 day), and Decay-3 (from lag 28 to lag 38 day. Composite analyses of circulation and temperature were performed for each period.

b. East Asian temperature during the Growth phase of the WSV event

Figure 4 represents the circulation and temperature anomalies during the Growth phase (from lag −16 to lag −6 day) of the WSV event. During this phase, positive and negative Z anomalies in the lower stratosphere (50 hPa) are located in North America and Eurasia, respectively. This circulation structure breaks and weakens dynamically a climatological stratospheric polar jet.
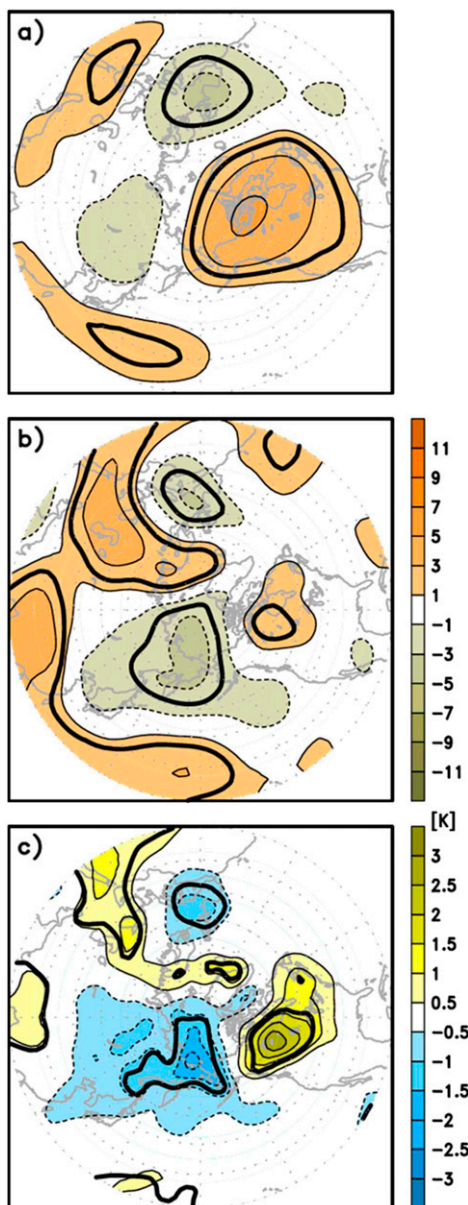
FIG. 4. Composite maps of normalized Z anomalies at (a) 50 and (b) 300 hPa, and (c) the temperature anomaly at 850 hPa during the Growth phase of a WSV event. The thick black line is the 95% confidence level.

The breaking of the stratospheric vortex is mainly caused by an upward-propagating stationary wave from the troposphere into the stratosphere (Matsuno 1970; Plumb 1985; Andrews et al. 1987). Recent studies have proposed the existence of tropospheric precursor patterns, such as a positive Z anomaly over northern Europe and a negative Z anomaly over the North Pacific (Garfinkel et al. 2010; Kolstad and Charlton-Perez 2011; Cohen and Jones 2011; Woo et al. 2015). In this study, these tropospheric precursor patterns are evident during

the Growth phase of the WSV event because this phase covers the preconditioning period during which upward propagation of a tropospheric wave weakens the stratospheric polar vortex.

Another interesting feature of the Growth phase is an East Asian cold anomaly, although it is weak (Fig. 4c). The cold signal may be caused dynamically by the precursor pattern (Cohen et al. 2002). The upper-tropospheric strong Z anomaly over northern Europe, including the Ural Mountains (one of the precursor patterns), can also play a role as a wave forcing; therefore, a negative Z anomaly may develop in its downstream region, such as East Asia (Honda et al. 2009; Wang et al. 2010; Cheung et al. 2013). In fact, the negative Z anomaly centered in the Bering Sea expands to East Asia (Fig. 4b). The expansion of the Z anomaly to East Asia could be partly contributed by a wave response to the strong anomaly over the Ural Mountains. As discussed earlier, the negative upper-level Z anomaly over East Asia implies that the EAT deepens and shifts westward as compared to its climatological strength and location. The strengthening of the EAT induces dynamically to lower-level cold air advection over East Asia (Boyle and Chen 1987; Jeong et al. 2005; Wang et al. 2009; Woo et al. 2012). Therefore, the cold conditions in East Asia during the Growth phase are strongly connected to the tropospheric precursor pattern of the WSV event. These results are consistent with previous studies that propose the high pressure over northwestern Eurasia and deepening of EAT may be one of the precursors of WSV occurrence (Cohen et al. 2007; Kolstad and Charlton-Perez 2011; Cohen and Jones 2011).

To examine the relation between the anticyclone anomaly over the Ural Mountains and the further deepening of the EAT, we examined the vertical structure of circulation over Eurasia in the lag interval of 2 days (Fig. 5). The positive Z anomaly develops abruptly after lag −12 day, and remains quasi stationary. In the meantime, the negative Z anomaly over East Asia starts to grow in the downstream region with the development of the Ural Mountains high anomaly and is strengthened until lag −6 day. Also, since lag −10 day, these anticyclone and cyclone anomalies appear clearly from the surface to the upper troposphere and lower stratosphere, respectively. This pattern is one of the well-known preconditions (see Fig. 8 in Cohen et al. 2014). These precondition features may imply that the deepening of EAT is strongly influenced by the upstream anticyclone anomaly. Another interesting feature is that the negative Z anomaly at the lower stratosphere exists over East Asia, albeit not significantly (Fig. 4a). The stratospheric anomaly is clearly connected to the tropospheric negative anomaly signal since lag −8 day (Figs. 5e,f). This connection between stratospheric and tropospheric circulation is strengthened
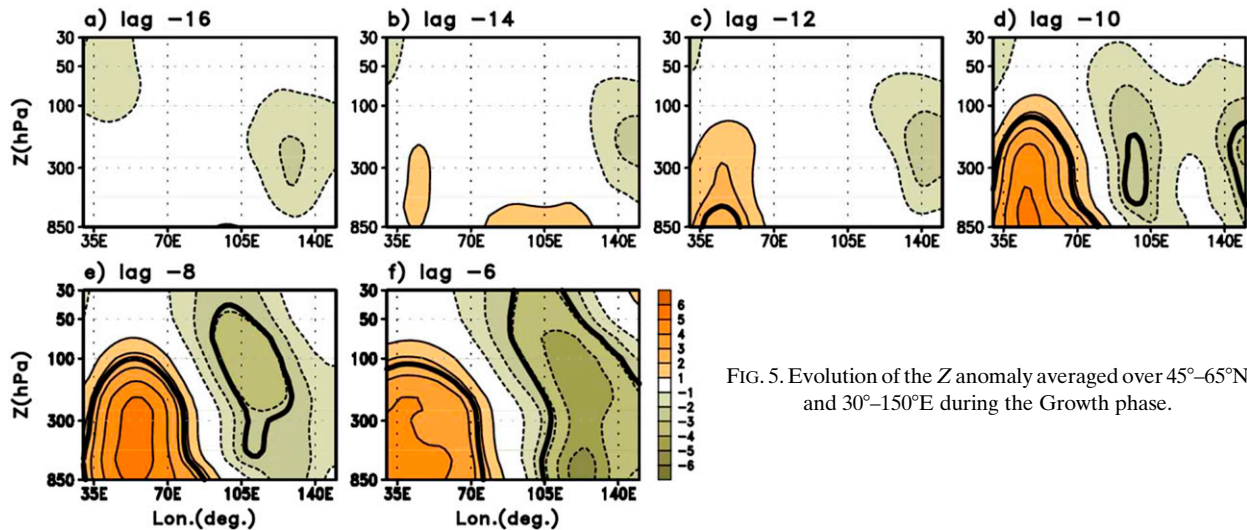
FIG. 5. Evolution of the Z anomaly averaged over 45°–65°N and 30°–150°E during the Growth phase.

over time; this feature implies that the tropospheric circulation starts to couple to the stratosphere before the onset of a WSV event. It is hard to conclude whether this connection is originated from the regional downward signal of stratospheric anomalies. Nevertheless, the connection between the negative Z anomaly, inducing the East Asian cold condition, and stratospheric circulation at lag −8 day before the onset of WSV event is an interesting observation.

c. Extreme cold over East Asia during the Peak phase

The cold signal over East Asia develops strongly during the Peak phase. In this section, we investigate the cause of the extreme cold anomaly during this phase. During the Peak phase, the positive Z anomalies in the lower stratosphere are strengthened over the polar cap region, and the negative Z anomalies are clear in midlatitudes but relatively weaker than the positive signal over the polar cap region (Fig. 6). Interestingly, the negative Z anomalies are remarkable over East Asia. In the upper troposphere, the overall pattern of Z anomalies is similar to that in the stratosphere, which is positive over the polar region and negative in midlatitude regions; that is, the vertical structure is generally barotropic in the stratosphere and troposphere. However, the zonally asymmetric components are stronger in the troposphere than those in the stratosphere. The strong positive Z anomaly over the polar cap region is elongated toward the North Pacific and Atlantic in the troposphere; this pattern suggests that the downward signal from the stratosphere is relatively strong in these regions. The remarkable feature at midlatitudes is that the deepening of the EAT in the upper troposphere was stronger than

during the Growth phase. This difference results in extremely cold conditions over East Asia during the Peak phase, as opposed to the Growth phase.

To examine the cause of the deepening of the EAT during this period, we checked the vertical structure of the circulation over Eurasia in time intervals of 2 days (Fig. 7). The Ural Mountains anticyclonic anomaly is abruptly weakened after lag −5 day, and its signal almost disappears after lag −1 day, whereas the cyclonic anomaly over East Asia is slightly strengthened from lag −5 to lag −3 day and persists significantly until lag +1 day, even though its strength is slightly weakened after lag −1 day. Considering the general time lag of the relationship between the EAT and circulation over the Ural Mountains, the lag correlation between the Z anomaly over Ural Mountains and East Asia shows a negative peak at lag 3 day (not shown); the tendency of the East Asian cyclonic anomaly can be explained by a wave response from the variation of the Ural Mountains Z anomaly. In other words, the Ural Mountains anticyclone anomaly as wave forcing still influences the intensification of EAT during the Peak phase, which induces the strong cold conditions. These features are also one of the well-known precursor patterns of the WSV events (Kolstad and Charlton-Perez 2011; Cohen and Jones 2011).

Nevertheless, the mean strength of the negative Z anomaly over East Asia during the Peak phase is stronger than the positive Z anomaly over the Ural Mountains (Fig. 6b). The strengthening of the negative Z anomaly (i.e., deepening of EAT) during the Peak phase may also be related to regional coupling with the stratospheric circulation over East Asia. From lag −5 to −3 day, the cyclonic anomaly over East Asia is
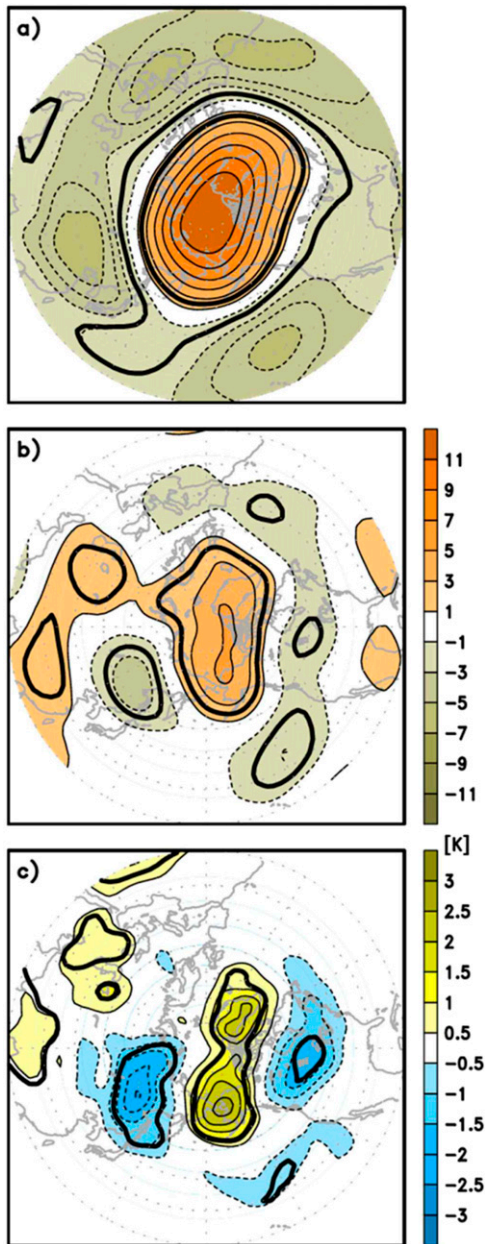
FIG. 6. Composite maps of normalized Z anomalies at (a) 50 and (b) 300 hPa, and (c) the temperature anomaly at 850 hPa in the Peak phase of a WSV event. The thick black line is the 95% confidence level.

strengthened in the lower stratosphere and upper troposphere despite the weakening of the Ural Mountains anticyclonic anomaly. The intensification in the lower stratosphere is especially remarkable. Moreover, the stratospheric negative Z anomaly over East Asia has already been strongly coupled with the EAT since lag −5 day before the onset of the WSV event. This coupling was strong until lag −1 day; then, it is weakened

after lag +1 day. These features suggest that the stratospheric circulation can be regionally coupled with the variation of the tropospheric circulation after lag −5 day. However, these results do not confirm the stratospheric impact on the tropospheric circulation. It is likely possible that the signals in both the stratosphere and troposphere may just vary together in a coupled relationship and the tropospheric circulation just impacts the stratospheric circulation. Therefore, it is hard to conclude the direct impact of the stratospheric circulation on the deepening of EAT in the Peak phase.

To examine the contribution of the stratospheric circulation to the deepening and persistence of the EAT, we tried to exclude the impact of the Ural Mountains high anomaly. The East Asian temperature in the Peak phase of WSV events is significantly correlated ($r = -0.47$) with the Ural Mountains Z anomaly in the precondition of WSV events (Fig. 8). This correlation indicates that the Ural Mountains high anomaly is partly responsible for the deepening of the EAT. However, in several cases, the EAT deepens in the absence of a strong Ural Mountains high anomaly. We selected WSV events with values less than -0.5 standard deviation (-36.23 m) of the EAT index and then divided them into two groups according to whether the Ural Mountains high anomaly is strong or not [larger or smaller than its 0.5 (46.38 m) standard deviation]. Then we compared the 16 events with strong Ural Mountains anticyclone anomalies (SUral case) with the 9 cases with the deep EAT and weak Ural Mountains high anomaly (WUral case) (Fig. 9). In the SUral case, the positive Z anomalies are strong over the Ural Mountains area by definition. In addition, the strong negative Z anomalies are distinctive, and indicate a deepening of the EAT (Fig. 9b). These features may be partly interpreted to be a result of wave propagation from the anticyclone over the Ural Mountains area. In the WUral cases, strong negative Z anomalies over East Asia appear despite insignificant Z anomalies over the Ural Mountains area (Fig. 9d). This result implies that the strong deepening of the EAT during the Peak phase is possible despite the weak wave forcing in the upstream region.

What make the strong negative Z anomaly in the WUral cases? Interestingly, in both cases, the stratospheric negative Z anomaly is also strong over East Asia (Figs. 9a,c). These stratospheric negative anomalies are also connected to the tropospheric negative Z anomaly over East Asia. Even though this feature cannot show the impact of the stratosphere on the tropospheric circulation, it can suggest a possibility that the regional coupling between the stratosphere and troposphere over East Asia is associated with the deepening of EAT. However, to demonstrate clearly the stratospheric impact
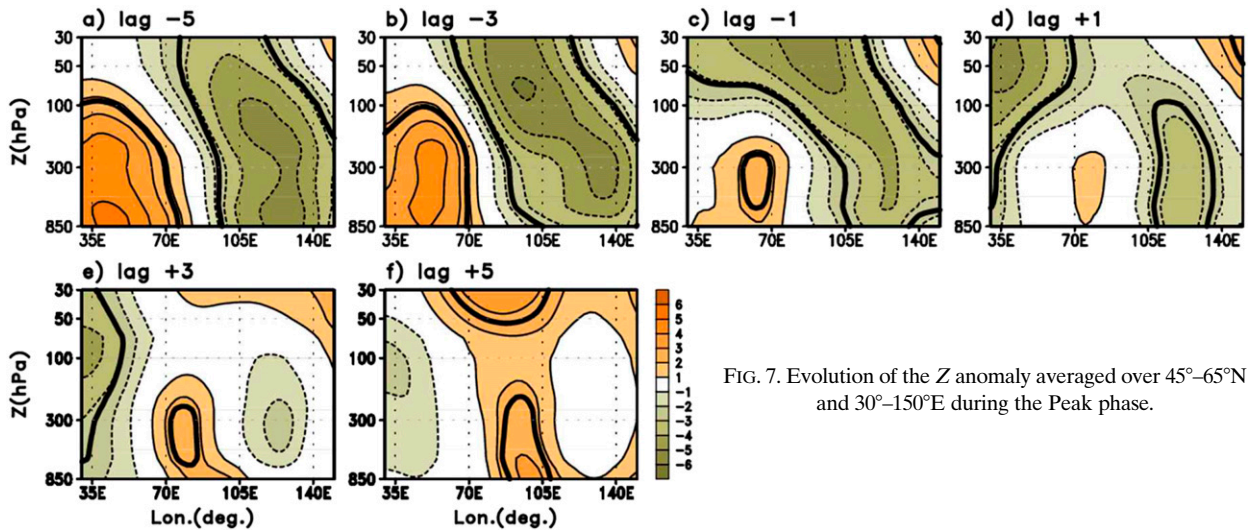
FIG. 7. Evolution of the Z anomaly averaged over 45°–65°N and 30°–150°E during the Peak phase.

on the EAT during the WSV events, further investigation on the dynamic process involved is required; we leave this for future study.

d. Weakening of cold anomaly over East Asia during Decay-1 phase

After the Peak phase, the cold signal over East Asia is rapidly weakened during the Decay-1 phase (Fig. 3a). To understand this distinctive change, the composite of circulation and temperature anomalies during this phase was examined (Fig. 10). The positive Z anomalies in the stratosphere are still strong over the polar region (Fig. 10a). However, compared to that in the Peak phase, the positive stratospheric Z anomaly in the Decay-1 period seems to rotate clockwise (Figs. 6a and 10a). The stratospheric rotation is strongly connected with the westward migration of Z anomaly in the upper troposphere. The positive Z anomaly over the North Pacific in the upper troposphere is elongated to the Atlantic during the Peak phase and seems to migrate westward to East Asia during the Decay-1 phase (Fig. 10b). Moreover, the negative Z anomalies over the northeastern Pacific in the Peak phase (Fig. 6b) seem to move to the central Pacific (Fig. 10b); this movement implies westward propagation of the circulation pattern from the Peak phase to the Decay-1 phase. Because of the approach of the positive Z anomaly from the North Pacific to East Asia, the strong negative Z anomaly during the Peak phase over East Asia is weakened rapidly in the Decay-1 phase. This circulation change results in the weakening of cold temperature anomalies over East Asia.

To show clearly the feature of westward propagation, the longitudinal evolution of the Z anomaly averaged

over 50°–70°N at 50 (Fig. 11a) and 300 hPa (Fig. 11b) is examined. In the upper troposphere, a distinctive negative Z anomaly is located over 100°–150°E during the Peak phase, and a strong positive Z anomaly appears over the North Pacific (180°–150°W). This positive Z anomaly moves westward (toward East Asia) over time, although it is gradually weakened. As the positive Z anomalies approach East Asia, the negative Z
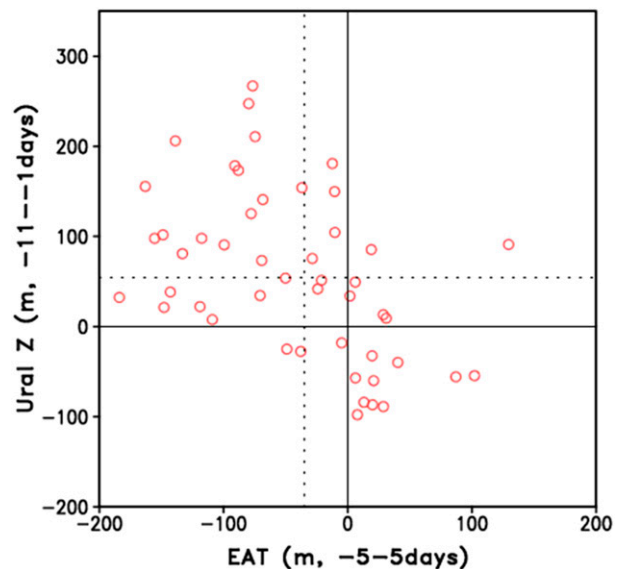

FIG. 8. Scatterplot on the relationship between the Ural Mountains Z index averaged (over 45°–65°N, 35°–70°E) during the 11 days before the onset of a WSV event and the EAT index averaged (over 45°–65°N, 105°–140°E) during the Peak phase. The horizontal dotted line is half the standard deviation of the Ural Mountains Z index; the vertical dotted line is half the standard deviation of the EAT index.
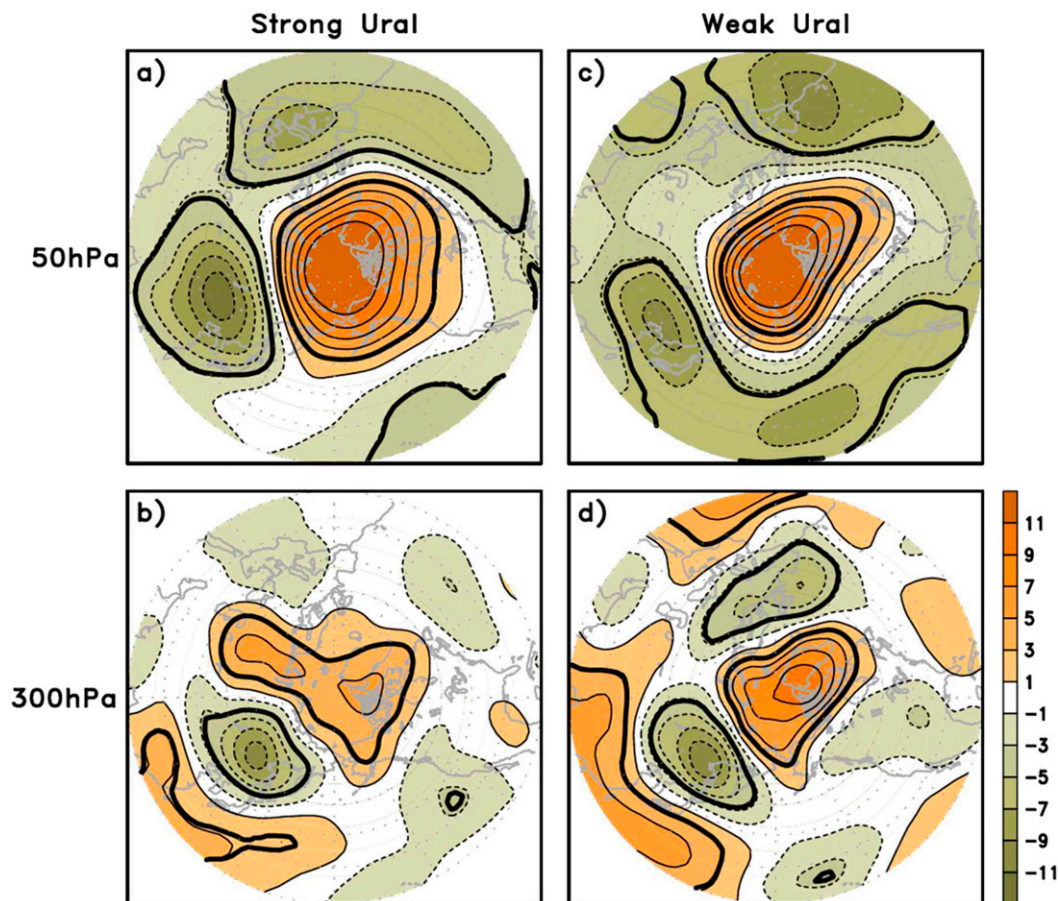
Strong Ural **Weak Ural**

FIG. 9. Composite maps of normalized Z anomalies at (a),(c) 50 and (b),(d) 300 hPa during the Peak phase of (left) SUral and (right) WUral WSV cases. The thick black line is the 95% confidence level.

anomalies in East Asia during the previous phase are weakened rapidly, and this leads to the weakening of cold anomalies over East Asia. Interestingly, the propagation in the lower stratosphere seems to precede the tropospheric circulation slightly, implying the stratospheric circulation leads to the tropospheric circulation. This feature indicates that the stratospheric downward signal continuously influences the tropospheric circulation from the North Pacific to East Asia, and the weakening of the EAT (corresponding to weakening of East Asian cold condition) in the Decay-1 phase is explained by the modulation of regional tropospheric circulation by the change in stratospheric circulation.

This westward propagation of the Z anomaly may be interpreted as a Rossby wave propagation, which is a basically an absolute vorticity conserving motion in the barotropic atmosphere. If an original perturbation vorticity exists, a motion is induced to conserve the absolute vorticity. This motion by the change in the vorticity field constitutes the Rossby wave propagation. The

conservation of absolute vorticity can be rewritten as a prognostic equation for relative vorticity ζ:

$$\frac{\partial \zeta}{\partial t} = -\mathbf{V}' \cdot \nabla\overline{\zeta} - \overline{\mathbf{V}} \cdot \nabla\zeta' - \mathbf{V}' \cdot \nabla\zeta' - \upsilon'\beta, \quad (3.1)$$

where $\mathbf{V}$ is a two-dimensional wind vector; the prime and overbar indicate the anomaly and winter season mean, respectively; β denotes the variation of Coriolis parameter f with latitude (df/dy); ∇ is the two-dimensional divergence operator; and υ is the meridional wind speed. We assumed that the flow is purely horizontal and barotropic.

In the midlatitudes, the nonlinear term [the third term on the right-hand side of Eq. (3.1)] is generally smaller than the other terms because the strength of the zonal wind anomaly is much smaller than its mean. However, this term is not negligible because the order of mean wind over the subpolar region, such as the Bering Sea, is similar to its anomaly. To examine whether the westward propagation of positive Z anomaly in the
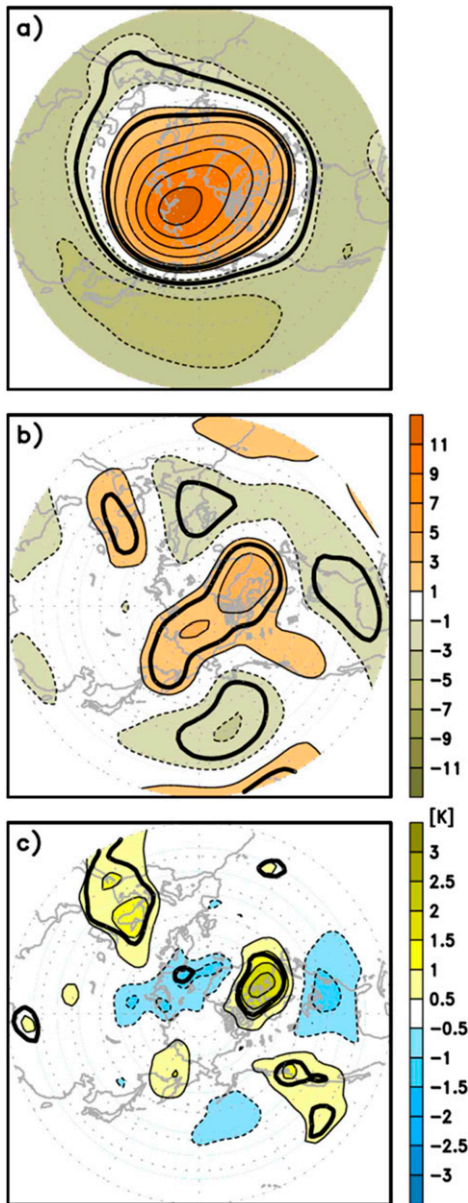
FIG. 10. Composite maps of normalized Z anomalies at (a) 50 and (b) 300 hPa, and (c) temperature anomaly at 850 hPa in the Decay-1 phase of a WSV event. The thick black line is the 95% confidence level.

FIG. 11. A lead–lag composite of the Z anomaly at (a) 50 and (b) 300 hPa, and (c) the tendency of relative vorticity at 300 hPa averaged over 50°–70°N before and after the onset of a WSV event (lag 0). The thick black line is the 95% confidence level.

Decay-1 phase follows the Rossby wave propagation mechanism, we calculated the tendency of relative vorticity and averaged the lag composite of relative vorticity tendency over 50°–70°N at 300 hPa between lag −10 and lag 10 day. Compared between the motion (moving of Z anomaly) and the tendency of relative vorticity, the negative tendency precedes the Z anomaly in its western side, and this feature appears continuously from the Bering Sea to East Asia between lag −5 and lag 10 day. The negative tendency on the western side of the
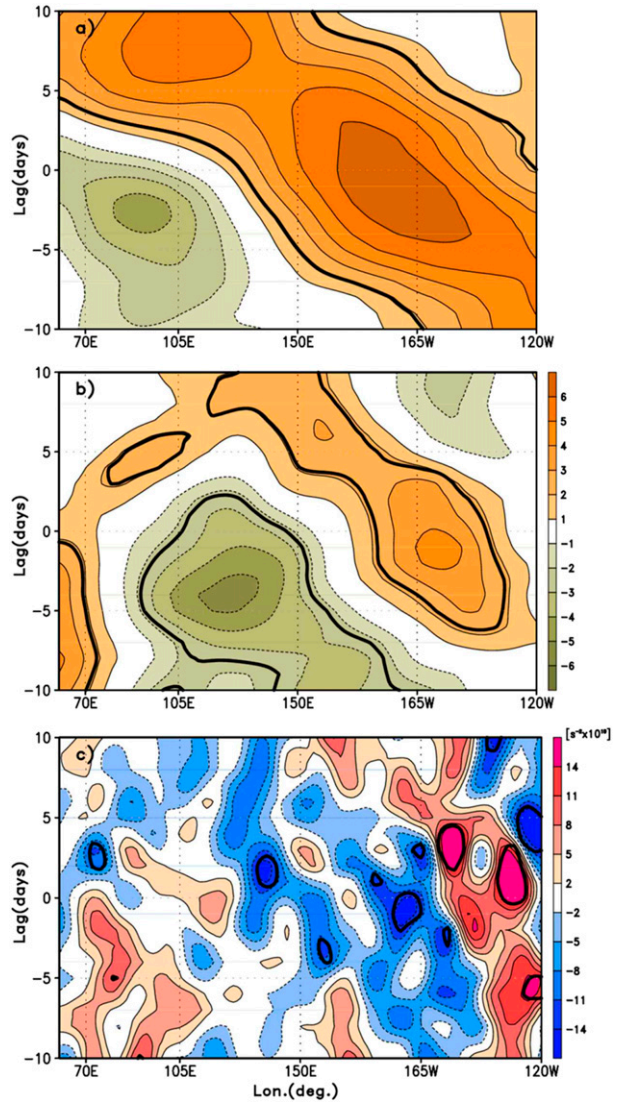
original perturbation means that the original perturbation propagates westward to conserve the absolute vorticity; this means that some of the westward propagation of the positive Z anomaly between lag −5 and lag 10 day can be explained by Rossby wave propagation.

e. Restrengthening of cold anomaly over East Asia during Decay-2 phase

East Asian cold anomalies significantly restrengthened during the Decay-2 phase (Fig. 12c). To understand this change, we examined the circulation and temperature patterns during this phase. The zonally asymmetric circulation pattern and the strength of the WSV in the
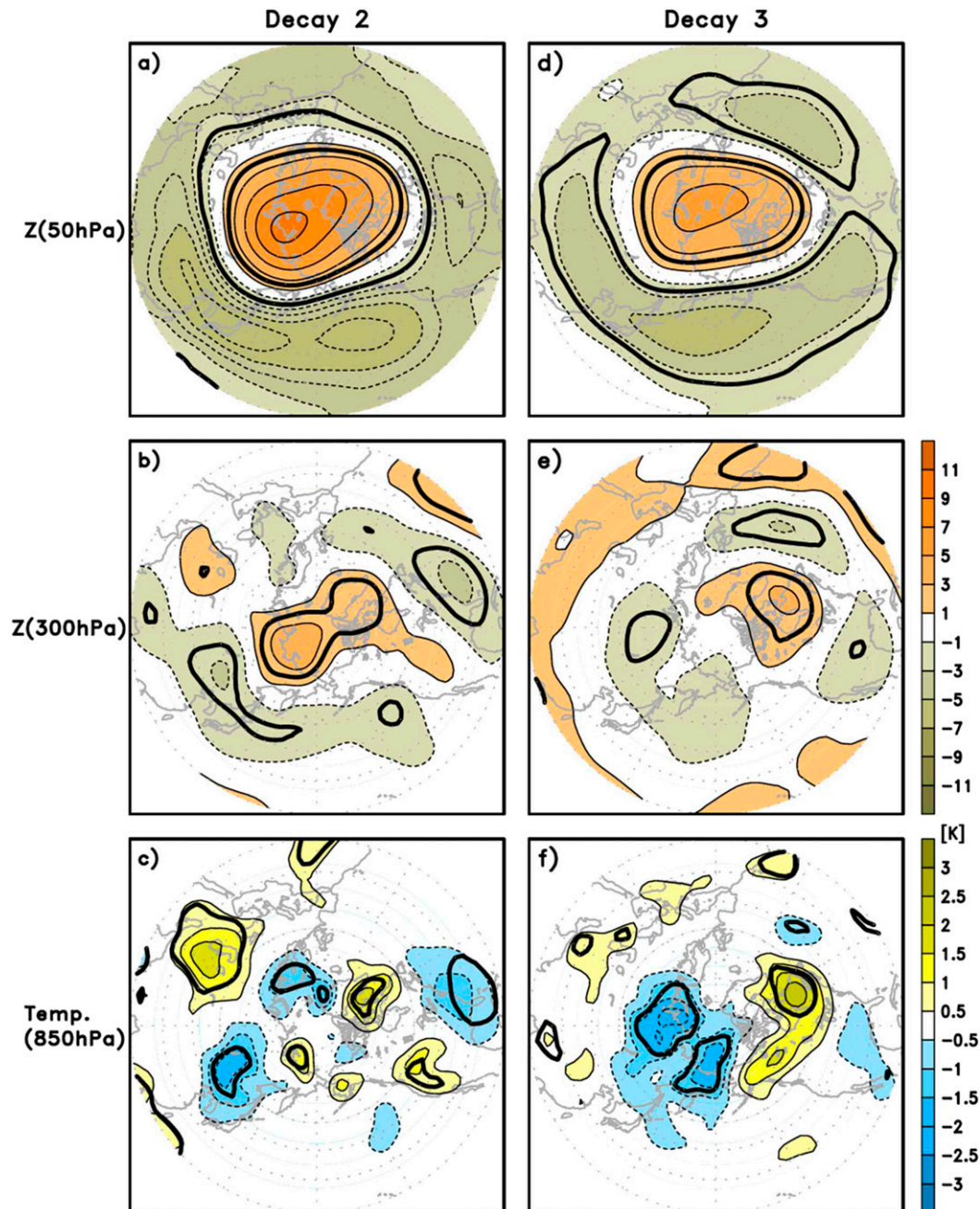
FIG. 12. Composite maps of normalized Z anomalies at (a),(d) 50 and (b),(e) 300 hPa, and (c),(f) the temperature anomaly at 850 hPa in the (left) Decay-2 phase and (right) Decay-3 phase of a WSV event. The thick black line is the 95% confidence level.

Decay-2 phase remain similar to those in the Decay-1 phase (Fig. 10). In spite of the similar WSV patterns occupied in the stratosphere (Fig. 12a), the negative Z anomaly in the upper troposphere is strengthened again over East Asia (Fig. 12b); this change may lead to the cold advection over East Asia at the lower level in the Decay-2 phase (Fig. 12c).

The reemergence of deepened EAT during the Decay-2 phase is likely to be related to the upper-tropospheric wave train propagated from the North Atlantic. Previous studies noted that the upper-tropospheric wave train that originated in the Atlantic is nonstationary and propagates eastward, interacting with the lower-tropospheric circulation and resulting in the intensification

of the Siberian high and East Asian cold anomaly after about a week (Joung and Hitchman 1982; Takaya and Nakamura 2005; Lu and Chang 2009; Sung et al. 2010). In particular, Sung et al. (2010) addressed that the downstream wave train develops in the persistent negative phase of the North Atlantic Oscillation (NAO). As shown in the upper-tropospheric circulation during the Decay-1 (Fig. 10b) and Decay-2 phases (Fig. 12b), the NAO-like circulation that appeared in the Decay-1 phase lasts over the Atlantic sector after the Decay-1 phase, and the wave train that originated from the North Atlantic (Greenland) develops over Eurasia in the Decay-1 phase, propagating eastward (Fig. 10b) until this wave train reaches East Asia in the Decay-2 phase (Fig. 12b), intensifying the EAT. This upper-tropospheric pattern is very similar to the patterns depicted in previous studies [see Fig. 3 in Takaya and Nakamura (2005) and Fig. 3 in Sung et al. (2010)]. Therefore, eastward propagation of a large-scale wave packet originating from the Atlantic, which is intrinsic to the internal tropospheric process, and its delayed influence on the East Asian region could be a possible explanation on the reemergence of deepened EAT and the East Asian cold anomaly in the Decay-2 phase.

During the Decay-3 phase, the circulation features in the stratosphere and troposphere are similar to those in the Decay-2 phase, but the intensity of stratospheric circulation anomalies is weakened conspicuously (Fig. 12d). Therefore, the anomalous circulation in the troposphere is less apparent than in the previous phases (Figs. 12b,e). Associated with the weakened circulation intensity, the cold anomaly over East Asia is also weak (Fig. 9f).

4. Summary and discussion

In this study, we examined the circulation change and its related temperature variation over East Asia during a WSV event. In particular, the temporal evolution of the circulation and temperature in the life cycle of the WSV events is focused. We found that the lower-tropospheric temperature over East Asia during the WSV events considerably fluctuates with a time scale longer than the synoptic scale, despite the gradual variation of stratospheric circulation and general negative AO phase during the WSV events. Specifically, the East Asian cold condition started in the Growth phase of WSV events. This cold condition is intensified during the Peak phase, is suddenly weakened during the Decay-1 phase, and is restrengthened during the Decay-2 phase.

This fluctuation of the lower-tropospheric temperature is strongly related to the variation of climatological EAT represented by the strong negative Z anomaly over East Asia in the upper troposphere. During the Growth phase, the weak deepening of EAT seems to be caused by the downstream wave response of the Ural Mountains anticyclone anomaly, which is well-known to be a precondition pattern for WSV events. This Ural Mountains anticyclone anomaly still strongly contributed to the deepening of EAT during the Peak phase. However, it is obvious that the EAT is regionally coupled with the stratospheric negative Z anomaly from lag -5 days before the onset of WSV events, though the coupling signal is strong before the onset of WSV events. Also, the deepening of EAT coupled with the stratospheric circulation is still distinctive in the case of the weak Ural Mountains anticyclone; this result implies that deepening of EAT during the Peak phase may be related to not only the response to wave forcing in the upstream region but also the regional coupling between the stratosphere and troposphere over East Asia.

After the Peak phase, the cold anomalies over East Asia significantly weakened in the Decay-1 phase despite the negative AO-like pattern in the troposphere. This feature is strongly related to the weakening of EAT by the westward-propagating signal of the positive Z anomaly connected with the stratospheric circulation from the North Pacific to East Asia. These results indicate that the regional temperature variation over East Asia is influenced by the regional circulation change related to stratospheric disturbance. During the Decay-1 phase, the eastward propagation of a large-scale wave packet originating from a negative NAO-like structure over the Atlantic Ocean is also remarkable over Eurasia. This wave train reaches East Asia during the Decay-2 phase, and its influence on the East Asian region can explain the reemergence of the deepened EAT and East Asian cold anomaly in the Decay-2 phase.

Although we showed a possible linkage between the stratosphere and troposphere on the variation of EAT during the life cycle of the WSV events, the dynamical mechanism of the simultaneous coupling is not clear. In particular, we suggest the possibility of a contribution to the deepening of EAT during the Peak phase by the coupling between the stratosphere and troposphere, but the tropospheric signal may also contribute to the stratospheric cyclonic circulation over East Asia. This possibility should be investigated further.

Nevertheless, our study emphasizes the evolution of tropospheric regional responses connected to a stratospheric disturbance, whereas previous studies focused on the tropospheric AO response associated with the WSV event (Baldwin and Dunkerton 2001; Thompson et al. 2002; Ambaum and Hoskins 2002; Limpasuvan et al. 2004). Even though the stratospheric signal changes monotonically, we showed that the tropospheric

responses, particularly regional responses, are somewhat complicated. We also suggested that a zonally asymmetric signal from the stratosphere to the troposphere and its related tropospheric process can lead to regionally different impacts of the WSV. For example, during the Peak phase, the positive Z anomalies are elongated toward the North Pacific and North Atlantic (Fig. 6b) where synoptic–eddy feedback is strong (Kug and Jin 2009) despite the zonally symmetric stratospheric anomalies. This elongation implies that downward signals from the stratosphere may be strong in particular regions. Once the zonally asymmetric pattern is induced in the troposphere, the tropospheric circulation is subjected to adjustment processes, such as regional amplification and wave propagation. The westward-propagating signal from the Peak phase to the Decay-1 phase seems to be understood as a part of this adjustment process. Also, we noted that the reemergence of the East Asian cold condition in the Decay-2 phase could be explained by the delayed impact of an eastward wave train originating from a persistent negative NAO-like structure over the Atlantic Ocean after the Decay-1 phase. The NAO-like circulation may be interpreted as the Atlantic feature of the tropospheric AO-like response of the WSV. Actually, the tropospheric circulation related to the WSV in the Decay-1 phase is regionally strong over the Atlantic sector (Fig. 10b). Therefore, the wave train crossing Eurasia during the Decay-1 and Decay-2 phases may also be comprehended as an intrinsic tropospheric process related to the WSV. In other words, the variation of EAT and temperature anomaly in the life cycle of WSV events may be explained by a regionally asymmetric coupling of WSV and its related tropospheric process.

Although the dynamical process of the coupling between the stratosphere and troposphere and its regional tropospheric adjustment should be addressed, the results of the regional variation in East Asia during the life cycle of WSV events will be useful for seasonal predictions based on the variability of the stratospheric polar vortex.

REFERENCES

Ambaum, M. H. P., and B. J. Hoskins, 2002: The NAO troposphere–stratosphere connection. *J. Climate,* **15,** 1969–1978, doi:10.1175/1520-0442(2002)015<1969:TNTSC>2.0.CO;2.

Andrews, D. G., J. R. Holton, and C. B. Leovy, 1987: *Middle Atmosphere Dynamics.* International Geophysics Series, Vol. 40, Academic Press, 489 pp.

Baldwin, M. P., and T. J. Dunkerton, 1999: Propagation of the Arctic Oscillation from the stratosphere to the troposphere. *J. Geophys. Res.,* **104,** 30 937–30 946, doi:10.1029/1999JD900445.

——, and ——, 2001: Stratospheric harbingers of anomalous weather regimes. *Science,* **294,** 581–584, doi:10.1126/science.1063315.

——, and D. W. J. Thompson, 2009: A critical comparison of stratosphere–troposphere coupling indices. *Quart. J. Roy. Meteor. Soc.,* **135,** 1661–1672, doi:10.1002/qj.479.

Black, R. X., 2002: Stratospheric forcing of surface climate in the Arctic Oscillation. *J. Climate,* **15,** 268–277, doi:10.1175/1520-0442(2002)015<0268:SFOSCI>2.0.CO;2.

——, and B. A. McDaniel, 2004: Diagnostic case studies of the northern annular mode. *J. Climate,* **17,** 3990–4004, doi:10.1175/1520-0442(2004)017<3990:DCSOTN>2.0.CO;2.

Boyle, J. S., and T.-J. Chen, 1987: Synoptic aspects of the wintertime East Asian monsoon. *Monsoon Meteorology, Oxford Monogr. Geol. Geophys.,* No. 7, C.-P. Chang and T. N. Krishnamurti, Eds., Oxford University Press, 125–160.

Butler, A. H., L. M. Polvani, and C. Deser, 2014: Separating the stratospheric and tropospheric pathways of El Niño–Southern Oscillation teleconnections. *Environ. Res. Lett.,* **9,** 024014, doi:10.1088/1748-9326/9/2/024014.

Charlton, A. J., and L. M. Polvani, 2007: A new look at stratospheric sudden warmings. Part I: Climatology and modeling benchmarks. *J. Climate,* **20,** 449–471, doi:10.1175/JCLI3996.1.

Cheung, H. N., W. Zhou, Y. Shao, W. Chen, H. Y. Mok, and M. C. Wu, 2013: Observational climatology and characteristics of wintertime atmospheric blocking over Ural–Siberia. *Climate Dyn.,* **41,** 63–79, doi:10.1007/s00382-012-1587-6.

Cohen, J., and J. Jones, 2011: Tropospheric precursors and stratospheric warmings. *J. Climate,* **24,** 6562–6572, doi:10.1175/2011JCLI4160.1.

——, D. Salstein, and K. Saito, 2002: A dynamical framework to understand and predict the major Northern Hemisphere mode. *Geophys. Res. Lett.,* **29,** 51-1–51-4, doi:10.1029/2001GL014117.

——, M. Barlow, P. J. Kushner, and K. Saito, 2007: Stratosphere–troposphere coupling and links with Eurasian land surface variability. *J. Climate,* **20,** 5335–5343, doi:10.1175/2007JCLI1725.1.

——, J. Furtado, J. Jones, M. Barlow, D. Whittleston, and D. Entekhabi, 2014: Linking Siberian snow cover to precursors of stratospheric variability. *J. Climate,* **27,** 5422–5432, doi:10.1175/JCLI-D-13-00779.1.

Colucci, S. J., 2010: Stratospheric influences on tropospheric weather systems. *J. Atmos. Sci.,* **67,** 324–344, doi:10.1175/2009JAS3148.1.

Ding, Y., and T. N. Krishnamurti, 1987: Heat budget of the Siberian high and the winter monsoon. *Mon. Wea. Rev.,* **115,** 2428–2449, doi:10.1175/1520-0493(1987)115<2428:HBOTSH>2.0.CO;2.

Domeisen, D. I. V., L. Sun, and G. Chen, 2013: The role of synoptic eddies in the tropospheric response to stratospheric variability. *Geophys. Res. Lett.,* **40,** 4933–4937, doi:10.1002/grl.50943.

Garfinkel, C. I., D. L. Hartmann, and F. Sassi, 2010: Tropospheric precursors of anomalous Northern Hemisphere stratospheric polar vortices. *J. Climate,* **23,** 3282–3299, doi:10.1175/2010JCLI3010.1.

Gong, D.-Y., and C.-H. Ho, 2002: The Siberian high and climate change over middle to high latitude Asia. *Theor. Appl. Climatol.,* **72,** 1–9, doi:10.1007/s007040200008.

Hartley, D. E., J. Villarin, R. X. Black, and C. A. Davis, 1998: A new perspective on the dynamical link between the strato-sphere and troposphere. *Nature,* **391,** 471–474, doi:10.1038/35112.

Hartmann, D. L., J. M. Wallace, V. Limpasuvan, D. W. J. Thompson, and J. R. Holton, 2000: Can ozone depletion and global warming interact to produce rapid climate change? *Proc. Natl. Acad. Sci. USA,* **97,** 1412–1417, doi:10.1073/pnas.97.4.1412.

Honda, M., J. Inoue, and S. Yamane, 2009: Influence of low Arctic sea-ice minima on anomalously cold Eurasian winters. *Geophys. Res. Lett.,* **36,** L08707, doi:10.1029/2008GL037079.

Jeong, J.-H., and C.-H. Ho, 2005: Changes in occurrence of cold surges over East Asia in association with Arctic Os-cillation. *Geophys. Res. Lett.,* **32,** L14704, doi:10.1029/2005GL023024.

——, ——, B.-M. Kim, and W.-T. Kwon, 2005: Influence of the Madden–Julian oscillation on wintertime surface air temper-ature and cold surges in east Asia. *J. Geophys. Res.,* **110,** D11104, doi:10.1029/2004JD005408.

——, B.-M. Kim, C.-H. Ho, D. Chen, and G.-H. Lim, 2006: Stratospheric origin of cold surge occurrence in East Asia. *Geophys. Res. Lett.,* **33,** L14710, doi:10.1029/2006GL026607.

Joung, C.-H., and M. H. Hitchman, 1982: On the role of suc-cessive downstream development in East Asian polar air outbreaks. *Mon. Wea. Rev.,* **110,** 1224–1237, doi:10.1175/1520-0493(1982)110<1224:OTROSD>2.0.CO;2.

Kalnay, E., and Coauthors, 1996: The NCEP/NCAR 40-Year Re-analysis Project. *Bull. Amer. Meteor. Soc.,* **77,** 437–471, doi:10.1175/1520-0477(1996)077<0437:TNYRP>2.0.CO;2.

Kim, B.-M., J.-H. Jeong, and S.-J. Kim, 2009: Investigation of stratospheric precursor for the East Asian cold surge using the potential vorticity inversion technique. *Asia-Pac. J. Atmos. Sci.,* **45,** 513–522.

Kodera, K., H. Mukougawa, and A. Fujii, 2013: Influence of the vertical and zonal propagation of stratospheric planetary waves on tropospheric blockings. *J. Geophys. Res. Atmos.,* **118,** 8333–8345, doi:10.1002/jgrd.50650.

Kolstad, E. W., and A. J. Charlton-Perez, 2011: Observed and simulated precursors of stratospheric polar vortex anomalies in the Northern Hemisphere. *Climate Dyn.,* **37,** 1443–1456, doi:10.1007/s00382-010-0919-7.

——, T. Breiteig, and A. A. Scaife, 2010: The association between stratospheric weak polar vortex events and cold air outbreaks in the Northern Hemisphere. *Quart. J. Roy. Meteor. Soc.,* **136,** 886–893, doi:10.1002/qj.620.

Kug, J.-S., and F.-F. Jin, 2009: Left-hand rule for synoptic eddy feedback on low-frequency flow. *Geophys. Res. Lett.,* **36,** L05709, doi:10.1029/2008GL036435.

Limpasuvan, V., D. W. J. Thompson, and D. L. Hartmann, 2004: The life cycle of the Northern Hemisphere sudden strato-spheric warmings. *J. Climate,* **17,** 2584–2596, doi:10.1175/1520-0442(2004)017<2584:TLCOTN>2.0.CO;2.

Lu, M.-M., and C.-P. Chang, 2009: Unusual late-season cold surges during the 2005 Asian winter monsoon: Roles of Atlantic blocking and the central Asian anticyclone. *J. Climate,* **22,** 5205–5217, doi:10.1175/2009JCLI2935.1.

Matsuno, T., 1970: Vertical propagation of stationary planetary waves in the winter Northern Hemisphere. *J. Atmos. Sci.,* **27,** 871–883, doi:10.1175/1520-0469(1970)027<0871:VPOSPW>2.0.CO;2.

——, 1971: A dynamical model of the stratospheric sudden warming. *J. Atmos. Sci.,* **28,** 1479–1494, doi:10.1175/1520-0469(1971)028<1479:ADMOTS>2.0.CO;2.

McDaniel, B. A., and R. X. Black, 2005: Intraseasonal dynamical evolution of the northern annular mode. *J. Climate,* **18,** 3820–3839, doi:10.1175/JCLI3467.1.

Mitchell, D. M., L. J. Gray, J. Anstey, M. P. Baldwin, and A. J. Charlton-Perez, 2013: The influence of stratospheric vortex displacements and splits on surface climate. *J. Climate,* **26,** 2668–2682, doi:10.1175/JCLI-D-12-00030.1.

Perlwitz, J., and N. Harnik, 2003: Observational evidence of a stratospheric influence on the troposphere by planetary wave reflection. *J. Climate,* **16,** 3011–3026, doi:10.1175/1520-0442(2003)016<3011:OEOASI>2.0.CO;2.

Plumb, R. A., 1985: On the three-dimensional propagation of sta-tionary waves. *J. Atmos. Sci.,* **42,** 217–229, doi:10.1175/1520-0469(1985)042<0217:OTTDPO>2.0.CO;2.

Polvani, L. M., and D. W. Waugh, 2004: Upward wave activity flux as a precursor to extreme stratospheric events and subsequent anomalous surface weather regimes. *J. Climate,* **17,** 3548–3554, doi:10.1175/1520-0442(2004)017<3548:UWAFAA>2.0.CO;2.

Qiu, Y. Y., and W. D. Wang, 1984: Progresses in the research of medium-range prediction of cold surge. *Proceedings of Medium Range Prediction of Cold Surge,* Peking University Press, 1–10.

Reichler, T., J. Kim, E. Manzini, and J. Kröger, 2012: A strato-spheric connection to Atlantic climate variability. *Nat. Geo-sci.,* **5,** 783–787, doi:10.1038/ngeo1586.

Rigor, I. G., R. L. Colony, and S. Martin, 2000: Variations in surface air temperature observations in the Arctic, 1979–97. *J. Climate,* **13,** 896–914, doi:10.1175/1520-0442(2000)013<0896:VISATO>2.0.CO;2.

Son, H.-Y., W. Park, J.-H. Jeong, S.-W. Yeh, B.-M. Kim, M. Kwon, and J.-S. Kug, 2012: Nonlinear impact of the Arctic Oscillation on extratropical surface air temperature. *J. Geophys. Res.,* **117,** D19102, doi:10.1029/2012JD018090.

Sung, M.-K., G.-H. Lim, and J.-S. Kug, 2010: Phase asymmetric downstream development of the North Atlantic Oscillation and its impact on the East Asian winter monsoon. *J. Geophys. Res.,* **115,** D09105, doi:10.1029/2009JD013153.

Taguchi, M., 2003: Tropospheric response to stratospheric sud-den warmings in a simple global circulation model. *J. Cli-mate,* **16,** 3039–3049, doi:10.1175/1520-0442(2003)016<3039:TRTSSW>2.0.CO;2.

Takaya, K., and H. Nakamura, 2005: Mechanisms of intraseasonal amplification of the cold Siberian high. *J. Atmos. Sci.,* **62,** 4423–4440, doi:10.1175/JAS3629.1.

Thompson, D. W. J., and J. M. Wallace, 1998: The Arctic Oscilla-tion signature in the wintertime geopotential height and temperature fields. *Geophys. Res. Lett.,* **25,** 1297–1300, doi:10.1029/98GL00950.

——, and ——, 2000: Annular modes in the extratropical cir-culation. Part I: Month-to-month variability. *J. Climate,* **13,** 1000–1016, doi:10.1175/1520-0442(2000)013<1000:AMITEC>2.0.CO;2.

——, M. P. Baldwin, and J. M. Wallace, 2002: Stratospheric con-nection to Northern Hemisphere wintertime weather: Impli-cations for prediction. *J. Climate,* **15,** 1421–1428, doi:10.1175/1520-0442(2002)015<1421:SCTNHW>2.0.CO;2.

Tomassini, L., E. P. Gerber, M. P. Baldwin, F. Bunzel, and M. Giorgetta, 2012: The role of stratosphere–troposphere

coupling in the occurrence of extreme winter cold spells over northern Europe. *J. Adv. Model. Earth Syst.,* **4,** M00A03, doi:10.1029/2012MS000177.

Wang, L., and W. Chen, 2010: Downward Arctic Oscillation signal associated with moderate weak stratospheric polar vortex and the cold December 2009. *Geophys. Res. Lett.,* **37,** L09707, doi:10.1029/2010GL042659.

——, ——, W. Zhou, and R. Huang, 2009: Interannual variations of East Asian trough axis at 500 hPa and its association with the East Asian winter monsoon pathway. *J. Climate,* **22,** 600–614, doi:10.1175/2008JCLI2295.1.

——, ——, ——, J. C. L. Chen, D. Barriopedro, and R. Huang, 2010: Effect of the climate shift around mid 1970s on the relationship between wintertime Ural blocking circulation and East Asian climate. *Int. J. Climatol.,* **30,** 153–158, doi:10.1002/joc.1876.

Woo, S.-H., B.-M. Kim, J.-H. Jeong, S.-J. Kim, and G.-H. Lim, 2012: Decadal changes in surface air temperature variability and cold surge characteristics over northeast Asia and their relation with the Arctic Oscillation for the past three decades (1979–2011). *J. Geophys. Res.,* **117,** D18117, doi:10.1029/2011JD016929.

——, M.-K. Sung, S.-W. Son, and J.-S. Kug, 2015: Connection between weak stratospheric vortex events and the Pacific decadal oscillation. *Climate Dyn.,* doi:10.1007/s00382-015-2551-z, in press.

Zhang, Y., K. R. Sperber, and J. S. Boyle, 1997: Climatology and interannual variation of the East Asian winter monsoon: Results from the 1979–95 NCEP/NCAR reanalysis. *Mon. Wea. Rev.,* **125,** 2605–2619, doi:10.1175/1520-0493(1997)125<2605:CAIVOT>2.0.CO;2.